A qualitative model for aggregation and diffusion of $$\beta $$ -amyloid in Alzheimer's disease

Yves Achdou, Bruno Franchi, Norina Marcello & Maria Carla Tesi

Journal of Mathematical Biology

ISSN 0303-6812
Volume 67
Combined 6-7

J. Math. Biol. (2014) 67:1369-1392
DOI 10.1007/s00285-012-0591-0

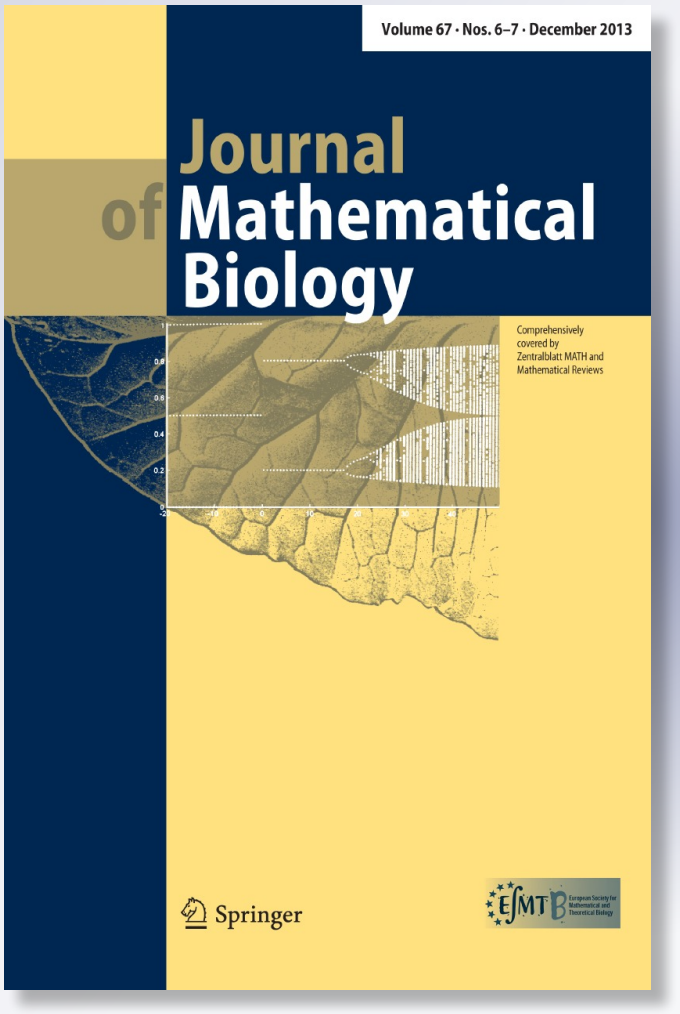

Springer

J. Math. Biol. (2013) 67:1369–1392
DOI 10.1007/s00285-012-0591-0

Mathematical Biology

A qualitative model for aggregation and diffusion of β-amyloid in Alzheimer's disease

Yves Achdou · Bruno Franchi · Norina Marcello · Maria Carla Tesi

Received: 2 March 2012 / Accepted: 5 September 2012 / Published online: 27 September 2012

Abstract In this paper we present a mathematical model for the aggregation and diffusion of Aβ amyloid in the brain affected by Alzheimer's disease, at the early stage of the disease. The model is based on a classical discrete Smoluchowski aggregation equation modified to take diffusion into account. We also describe a numerical scheme and discuss the results of the simulations in the light of the recent biomedical literature.

Keywords Alzheimer's disease · Smoluchowski equation · Diffusion equation

Mathematics Subject Classification (2000) 35F61 · 92B05 · 65M99

B.F. and M.C.T. are supported by MURST, Italy, and by University of Bologna, Italy, funds for selected research topics.

Y. Achdou
Laboratoire Jacques-Louis Lions, Sorbonne Paris Cité, Univ. Paris Diderot,
UPMC, CNRS, UMR 7598, 75205 Paris, France
e-mail: achdou@math.jussieu.fr

B. Franchi · M. C. Tesi (✉)
Dipartimento di Matematica, Università di Bologna,
Piazza di Porta S. Donato 5, 40127 Bologna, Italy
e-mail: mariacarla.tesi@unibo.it

B. Franchi
e-mail: bruno.franchi@unibo.it

N. Marcello
S.C. Neurologia, Azienda Ospedaliera Santa Maria Nuova-IRCCS,
Viale Risorgimento 80, 42123 Reggio Emilia, Italy
e-mail: marcello.norina@asmn.re.it

1 Introduction

This paper aims at proposing a mathematical model for the onset of the Alzheimer disease (AD hereafter), nowadays one of the most common late life dementia.

In recent years, mathematical models have been largely developed for the description and the study of other pathologies such as tumors. Restricting ourselves to the neurological area, we refer for instance to Hatzikirou et al. (2005). Concerning AD, modeling is far less developed. Besides the classical approaches *in vivo* and *in vitro*, there has been an increasing interest toward the approach *in silico*, i.e. toward mathematical modeling and computer simulations. We refer for instance to Urbanc et al. (1999); Cruz et al. (1997), and, first of all, to the remarkably exhaustive and deep paper (Edelstein-Keshet and Spiross 2002).

It is important to stress from the very beginning that, despite the large number of experimental data that can be extracted from biomedical literature and incorporated in mathematical models as in Edelstein-Keshet and Spiross (2002), mathematical models do not currently have a "predictive" value; rather, they are what physicists call "toy models", i.e. simplified formal models that can be used in order to test preliminary new theories, quickly identifying, for instance, the most relevant hypotheses or rejecting those less likely to lead to new insights. In this sense, qualitative models take a place beside more specific fully quantitative models, and can be used for reducing experimental costs or for overcoming structural difficulties.

The aim of this note is to provide an elementary mathematical model of the diffusion and agglomeration of the β-amyloid (Aβ hereafter) in the brain affected by Alzheimer's disease (AD). Current estimates of AD incidence are above 24 million of affected persons worldwide, a number that is expected to double every 20 years. For a comprehensive review of the key aspects of the disease, such as epidemiology, genetics, pathogenesis, diagnosis, and treatment, we refer for instance to Blennow et al. (2006) and Mattson (2004).

For a detailed review of the current knowledge on the role of Aβ in AD (the so-called *amyloid cascade hypothesis*), we refer to Haass and Selkoe (2007). Roughly speaking, Aβ is produced normally by the intramembranous proteolysis of APP (amyloid precursor protein) throughout life, but a change in the metabolism may increase the total production of Aβ, and, in particular, the production—among other isoforms—of the monomeric Aβ_{40} and Aβ_{42} that are highly toxic. From now on, for sake of simplicity, we shall simply write Aβ.

Successively, Aβ oligomers are subject to two different phenomena:

- agglomeration, leading eventually to the formation of long, insoluble amyloid fibrils, which accumulate in spherical microscopic deposits known as senile plaques;
- diffusion through the microscopic tortuosity of the brain tissue.

In fact, agglomeration can be articulated in several steps (Chimon et al. 2007): initial *seeds*, soluble small oligomers, protofibrils and insoluble polymers, amyloid fibrils with a β-sheet conformation. However, this level of description remains behind the scope of our model, as will be explained in detail in the next section.

We refer for instance to Walsh and Selkoe (2007) for an exhaustive historical account, and to Ono et al. (2009) for an experimental analysis of the different types of oligomers.

The plan of the work is the following:

- in Sect. 1, we describe the general biological context in which we will operate, and situate the model from a phenomenological point of view with useful bibliographical references;
- in Sect. 2, we give a detailed description of our model and particularly emphasize the specific phenomena that are taken into account and the relevant variables in our approach;
- in Sect. 3, we present some rigorous results on the mathematical model along with a bio-physical interpretation;
- in Sect. 4, we describe a numerical scheme in detail. In particular we explain some additional assumptions made in order to simplify the implementation;
- in Sect. 5, we present some numerical results and discuss them in view of some recent results from biomedical literature;
- in Sect. 6, we propose some conclusions and comments.

2 Description of the model

It has been recently suggested that *soluble* $A\beta$ can be considered as the principal cause of neuronal death and eventually of dementia (Walsh and Selkoe 2007). Indeed modern $A\beta$ enzyme-linked-immunosorbent assays (ELISAs) coupled with western blotting and mass spectrometry suggest that the plaque counting yields a poor measure of the severity of the AD, and that the levels of soluble $A\beta$, including soluble oligomers, correlate much better with the presence and degree of cognitive deficits than plaque statistics. Even more, quoting Haass and Selkoe (2007), *the idea that large aggregates of a disease causing protein can actually be inert or even protective to neurons has been supported by work on other protein folding disorders*. Therefore, in the present work, we are interested in considering the early stage of AD when small amyloid fibrils are free to move and to coalesce in the brain.

In addition, we discard deliberately fibril fragmentation, which can be considered as a secondary process in the mechanism of amyloid self-assembly (Knowles et al. 2009; Xue et al. 2008), especially when oligomers of small size are involved.

It is natural to describe the agglomeration phenomenon by means of the so-called Smoluchowski equations (classical references are Smoluchowski (1917) and Drake (1972); further recent references related to the present paper are listed below).

Since the fibrils at this stage are relatively small, diffusion also plays a key role in the description of the behaviours of the fibrils, as recently discussed e.g. in Meyer-Luhmann (2004); Meyer-Luehmann et al. (2008).

When attempting to produce a mathematical model, we have to fix a spatial scale once and for all. Thus, we consider a portion of the hippocampus or of the cerebral cortex (the regions of the brain mainly affected by AD) whose size is comparable to a multiple of the size of a neuron, and we avoid the description of intracellular

phenomena, as well as of the clinical manifestations of the disease at a macroscopic scale (see some additional comments on this in the final section).

With this choice of scale, it is coherent to assume that the diffusion is uniform, and therefore to model it by the usual Fourier linear diffusion equation. Indeed, if one considers a large (i.e. macroscopic) portion of the brain tissue, it has been recently proved that the diffusion of the amyloid is affected by the metabolic activity and therefore may change from one region to another according to the neuronal activity (Bero et al. 2011). On the contrary, since we focus on a small portion of the celebral tissue (typically the affected areas are the hippocampus or of the cerebral cortex), linear diffusion appears to be the most appropriate (see, for instance, Nicholson and Sykov (1998)).

Moreover, we assume that "large" assemblies do not aggregate with each other. This assumption is related to technical aspects of the model (basically, it is meant to prevent blow-up phenomena for solutions at a finite time), but also it is coherent with experimental data (see below).

The portion of cerebral tissue we consider is represented by a bounded smooth region $\Omega_0 \subset \mathbb{R}^3$ (since only qualitative information is desired we shall take $\Omega_0 \subset \mathbb{R}^2$ in our simulations for keeping the computing effort small enough), whereas the neurons are represented by a family of regular regions Ω_j such that

(1) $\overline{\Omega}_j \subset \Omega_0$ if $j = 1, \ldots, M$;
(2) $\overline{\Omega}_i \cap \overline{\Omega}_j = \emptyset$ if $i \neq j$.

We set

$$\Omega := \Omega_0 \setminus \bigcup_{j=1}^{M} \overline{\Omega}_i.$$

From the mathematical point of view, we will consider a vector-valued function $u = (u_1, \ldots, u_N)$, where $N \in \mathbb{N}$ and $u_j = u_j(t, x)$, $t \in \mathbb{R}$, $t \geq 0$ (the time), and $x \in \Omega$:

- if $1 \leq j < N - 1$, then $u_j(t, x)$ is the (molar) concentration at the time t at the point x of an Aβ assembly of j monomers;
- u_N takes into account aggregations of more than $N - 1$ monomers. Although u_N has a different meaning from the other u_m's, we keep the same letter u in order to avoid cumbersome notations.

The production of Aβ in the monomeric form at the level of neuron membranes is modeled by a non homogeneous Neumann condition on $\partial\Omega_j$, the boundary of Ω_j, for $j = 1, \ldots, M$. Finally, an homogeneous Neumann condition on $\partial\Omega_0$ is meant to artificially isolate our portion of tissue from its environment.

Thus, we are lead to the following Cauchy–Neumann problem

$$\begin{cases} \frac{\partial}{\partial t} u_1 = d_1 \Delta_x u_1 - u_1 \sum_{j=1}^{N} a_{1,j} u_j \\ \frac{\partial u_1}{\partial \nu} = \psi_0 \equiv 0 \quad \text{on } \partial\Omega_0 \\ \frac{\partial u_1}{\partial \nu} = \psi_j \quad \text{on } \partial\Omega_j,\ j = 1, \ldots, M \\ u_1(x, 0) = U_1(x) \geq 0, \end{cases} \tag{1}$$

where $0 \leq \psi_j \leq 1$ is a smooth function for $j = 1, \ldots, M$, describing the production of the amyloid near the membrane of the neuron.

Indeed, the production of Aβ is not uniformly distributed on the membrane of the neuron. Indeed, it has been observed that the plaque accumulates near the axon's outgrowth, in angular position with respect to the neuron's soma. A possible explanation of this phenomenon is that pathological changes in APP processing are concentrated in axons and synapses, since APP is normally transported within axons and its cleavage is regulated by sinaptic inputs (Mattson 2004).

In the mathematical model, this localization of the production is expressed by means of the choice of the functions ψ_j. Indeed, the ψ_j's are not constant or bounded away from zero on all the $\partial\Omega_j$'s (that would correspond to a uniform production of amyloid on the neuron membranes), but are identically zero except for a small portion of the boundary of the set Ω_j, that represents the portion of the membrane involved in the production of the amyloid. We refer to the introduction of Sect. 5 for a discussion related to the numerical simulation.

We only take into account neurons affected by the disease, i.e. we assume $\psi_j \not\equiv 0$ for $j = 1, \ldots, M$. Moreover, to avoid technicalities, we assume that U_1 is smooth, more precisely $U_1 \in \mathbf{C}^{2+\alpha}(\bar{\Omega})$ for some $\alpha \in (0, 1)$, and that $\frac{\partial U_1}{\partial \nu} = \psi_j$ on $\partial\Omega_j$, $j = 0, \ldots, M$.

In addition, if $1 < m < N$,

$$\begin{cases} \frac{\partial}{\partial t} u_m = d_m \Delta_x u_m - u_m \sum_{j=1}^{N} a_{m,j} u_j + \frac{1}{2} \sum_{j=1}^{m-1} a_{j,m-j} u_j u_{m-j}. \\ \frac{\partial u_m}{\partial \nu} = 0 \quad \text{on } \partial\Omega_0 \\ \frac{\partial u_m}{\partial \nu} = 0 \quad \text{on } \partial\Omega_j,\ j = 1, \ldots, M \\ u_m(x, 0) = 0, \end{cases} \tag{2}$$

and

$$\begin{cases} \frac{\partial}{\partial t} u_N = d_N \Delta_x u_N + \frac{1}{2} \sum_{j+k \geq N, k<N, j<N} a_{j,k} u_j u_k. \\ \frac{\partial u_N}{\partial \nu} = 0 \quad \text{on } \partial\Omega_0 \\ \frac{\partial u_N}{\partial \nu} = 0 \quad \text{on } \partial\Omega_j,\ j = 1, \ldots, M \\ u_N(x, 0) = 0, \end{cases} \tag{3}$$

where $d_j > 0$, $j = 1, \ldots, N$ and $a_{i,j} = a_{j,i} > 0$, $i, j = 1, \ldots, N$ (but $a_{N,N} = 0$).

For reasons related to the model, we can assume that the diffusion coefficients d_j are small when j is large, since big assemblies do not move. In fact, the diffusion coefficient of a soluble peptide scales approximately as a reciprocal of the cube root of its molecular weight (see Goodhill (1997) and also Nicholson and Sykov (1998)).

The justification of the condition $j, k < N$ in (3) requires a few more words. In fact, we must remember that the meaning of u_N differs from that of $u_m, m < N$, as well as the identity

$$\frac{1}{2} \sum_{j+k \geq N, k<N, j<N} a_{j,k} u_j u_k = \frac{1}{2} \sum_{j+k \geq N} a_{j,k} u_j u_k - u_N \sum_{j=1}^{N} a_{N,j} u_j. \tag{4}$$

The idea is that u_N should describe the sum of the densities of all the "large" assemblies. We assume that large assemblies exhibit all the same coagulation properties and do not coagulate with each other.

Let us briefly show how (3) is obtained: we start by writing the exact Smoluchowski equation for all $m \geq 1$ using $\tilde{u}_m$ instead of u_m in order to avoid confusion, i.e. nothing but the PDE in (2) with m ranging from 2 to ∞. We have

$$\frac{\partial}{\partial t}\tilde{u}_m = d_m \Delta_x \tilde{u}_m - \tilde{u}_m \sum_{j=1}^{\infty} a_{m,j}\tilde{u}_j + \frac{1}{2}\sum_{j=1}^{m-1} a_{j,m-j}\tilde{u}_j\tilde{u}_{m-j}, \tag{5}$$

where, coherently with our assumptions, we assume

(i) $d_m = d_N$ for $m \geq N$;
(ii) $a_{m,j} = a_{N,j}$ for $m \geq N$. In particular, if $m, j \geq N$, $a_{m,j} = a_{N,j} = a_{N,N} = 0$.

Therefore, if $m \geq N$, (5) becomes

$$\frac{\partial}{\partial t}\tilde{u}_m = d_N \Delta_x \tilde{u}_m - \tilde{u}_m \sum_{j=1}^{N-1} a_{N,j}\tilde{u}_j + \frac{1}{2}\sum_{j=1}^{m-1} a_{j,m-j}\tilde{u}_j\tilde{u}_{m-j}, \tag{6}$$

Now we sum up (6) for $m \geq N$, and we set for a while $v := \sum_{m\geq N} \tilde{u}_m$. We want to show precisely that v satisfies the Eq. (3) (satisfied by u_N). By i), we have

$$\begin{aligned}\frac{\partial v}{\partial t} &= d_N \Delta_x v - \sum_{m\geq N} \tilde{u}_m \sum_{j=1}^{N-1} a_{N,j}\tilde{u}_j + \frac{1}{2}\sum_{m\geq N}\sum_{i=1}^{m-1} a_{i,m-i}\tilde{u}_i\tilde{u}_{m-i} \\ &:= d_N \Delta_x v - I_1 + \frac{1}{2} I_2.\end{aligned}$$

It is clear that

$$I_1 = \sum_{m\geq N} \tilde{u}_m \sum_{j=1}^{N-1} a_{N,j}\tilde{u}_j = v \sum_{j=1}^{N-1} a_{N,j}\tilde{u}_j,$$

that is precisely the second term in (4), since $a_{N,N} = 0$.

As for I_2, if we set $j := i$ and $k := m - i$, we obtain the first term in (4). Finally, if set $u_m = \tilde{u}_m$ for $m < N$ and $u_N = v$ we recover the PDE in (3), as desired.

The diffusion-agglomeration system described above has been already considered in the literature (without reference to Aβ amyloid and to Alzheimer's disease) with homogeneous boundary Neumann conditions (see for instance Laurençot and Mischler (2002); Mischler and Ricard (2003); Amann (2000); Wrzosek (1997); Amann and Weber (2001); Amann and Walker (2005) and, for a numerical approach, Filbet and Laurençot (2004a,b); Bourgade and Filbet (2008)). Non-homogeneous boundary data on $\partial\Omega_j$, $j = 1, \ldots, N$, i.e. on the external membrane of the neurons, are crucial here, since they model the production of Aβ-monomers at the level of the membrane

itself. This, in turn, is an essential aspect of the phenomenon *in vivo*. Obviously, the non-homogeneous Neumann boundary conditions prohibits mass conservation; thus, some estimates provided in the literature in the homogeneous case fail to hold and we have to adapt the techniques of Wrzosek (1997) to our situation, relying on a repeated use of the classical parabolic maximum principle.

Usually, mathematical and physical literature refers to the equations appearing in (1), (2) and (3) as to a finite discrete Smoluchowski type system with diffusion. Originally, in Smoluchowski (1917), Smoluchowski introduced a system of infinite discrete differential equations (without diffusion) for the study of rapid coagulation of aerosols. Smoluchowski's theory was successively extended to cover different physical situations, and, in particular, a class of corresponding integro-differential equations was introduced for the study of the physics of clouds, where sums are replaced by integrals. We refer to Drake (1972) for a exhaustive historical account. We restrict ourselves to a *finite discrete* system since our model can be reduced to the study of only three kinds of particles with completely different bio-physical properties:

- Monomers, that are produced by neuronal membranes. Mathematically, this means that the diffusion-coagulation equation is coupled with non-homogeneous Neumann boundary conditions.
- Soluble oligomers, that diffuse in the brain and coagulate to form larger assemblies. Mathematically, this means that the diffusion-coagulation equation is coupled with homogeneous Neumann boundary conditions.
- Long fibrils, characterized by a very low diffusion, that do not coagulate with each other.

Applications of Smoluchowski equation to the description of the agglomeration of Aβ amyloid appear in Murphy and Pallitto (2000). In this paper, the authors compare experimental data, obtained *in vitro*, with numerical simulations based on Smoluchowski equation (without diffusion) in order to describe the process leading to insoluble fibril aggregates from soluble amyloid. The form of the coefficients $a_{i,j}$ (the coagulation rates) considered in Murphy and Pallitto (2000)—that is based on end-to-end association, consistently with our choice of restricting ourselves to primary structures—is stated in formula (13) therein (see also the comments following the formula). The physical arguments leading to formula (13) in Murphy and Pallitto (2000) rely on sophisticated statistical mechanics considerations (see also Hill (1983), Tomsky and Murphy (1992)).

In our numerical simulations, we use a slightly approximate form of these coefficients, taking

$$a_{i,j} = \alpha \frac{1}{ij}, \quad \text{where } \alpha > 0. \tag{7}$$

In fact, this approximation basically consists of neglecting logarithmic terms in front of linear ones for large i, j. It is clearly coherent with experimental data to assume $a_{N,N} = 0$ for large N. This is equivalent to saying that large oligomers do not aggregate with each other.

We stress again that the present model only takes into account the evolution of the Aβ, and ignores the role played by the microglia in neuronal death and in the formation

of senile plaques. For these aspects, we refer for instance to Meyer-Luehmann et al. (2008) and Edelstein-Keshet and Spiross (2002). In particular, if we identify senile plaques in our model with the sets $\{x \ : u_N(t,x) > c > 0\}$, our model leads to smooth shape of senile plaques, see the numerical simulations in Sect. 5, in disagreement with evidences found *in vivo*. This may be explained by Fig. 3 in Edelstein-Keshet and Spiross (2002) and related comments on the role of the microglia.

3 Rigorous mathematical results

We keep now the notations of the previous Section. Let $g \in \mathbf{C}^{2+\alpha}(\bar{\Omega})$ be such that

$$\frac{\partial g}{\partial \nu} = 0 \quad \text{on } \partial\Omega_0$$

and

$$\frac{\partial g}{\partial \nu} = \psi_j \quad \text{on } \partial\Omega_j,\ j = 1, \dots, M.$$

Set now $v_1 := u_1 - g$, $v_m := u_m$ for $m > 1$. Equations (1), (2), (3) become

$$\begin{cases} \frac{\partial}{\partial t} v_1 = d_1 \Delta_x v_1 - v_1\big(a_{1,1} v_1 + \sum_{j=2}^N a_{1,j} v_j + 2a_{1,1} g\big) \\ \qquad\qquad +d_1 \Delta_x g - a_{1,1} g^2 - g \sum_{j=2}^N a_{1,j} v_j \\ \frac{\partial v_1}{\partial \nu} = 0 \quad \text{on } \partial\Omega_0 \\ \frac{\partial v_1}{\partial \nu} = 0 \quad \text{on } \partial\Omega_j,\ j = 1, \dots, M \\ v_1(x,0) = U_1(x) - g(x), \quad x \in \Omega, \end{cases} \tag{8}$$

whereas when $1 < m < N$

$$\begin{cases} \frac{\partial}{\partial t} v_m = d_m \Delta_x v_m - v_m\big(\sum_{j=1}^N a_{m,j} v_j + a_{m,1} g\big) \\ \qquad\qquad +\frac{1}{2} \sum_{j=1}^{m-1} a_{j,m-j} v_j v_{m-j} + a_{1,m-1} g v_{m-1}. \\ \frac{\partial v_m}{\partial \nu} = 0 \quad \text{on } \partial\Omega_0 \\ \frac{\partial v_m}{\partial \nu} = 0 \quad \text{on } \partial\Omega_j,\ j = 1, \dots, M \\ v_m(x,0) = 0, \end{cases} \tag{9}$$

and

$$\begin{cases} \frac{\partial}{\partial t} v_N = d_N \Delta_x v_N + \frac{1}{2} \sum_{j+k \geq N} a_{j,k} v_j v_k \\ \qquad\qquad +g\big(a_{1,N-1} v_{N-1} + a_{1,N} v_N\big) \\ \frac{\partial v_N}{\partial \nu} = 0 \quad \text{on } \partial\Omega_0 \\ \frac{\partial v_N}{\partial \nu} = 0 \quad \text{on } \partial\Omega_j,\ j = 1, \dots, M \\ v_N(x,0) = 0. \end{cases} \tag{10}$$

Proposition 3.1 *There exists $\tau_{\max} > 0$ such that problem (8)–(10) has a local classical maximal solution $v \in \mathbf{C}^{1+\alpha/2, 2+\alpha}([0,\tau] \times \bar{\Omega})$ for every $\tau \in (0, \tau_{\max})$. Therefore, the same assertion holds for problem (1)–(3).*

Proof We apply Theorem 1 p. 111 (Rothe 1984) (see also Theorem 7.1 in the Appendix). □

Proposition 3.2 *If $u = (u_1, \ldots, u_N)$ is a solution of problems (1)–(3), then $u_m > 0$ in $(0, \tau_{\max}) \times \bar{\Omega}$ for $m = 1, \ldots, N$.*

Proof Let us argue by induction on m. If $m = 1$, by the comparison theorem Theorem 3 p.123 of Rothe (1984) (see also Theorem 7.2 in the Appendix), we obtain that either $u_1 \equiv 0$, or $u_1 > 0$. But u_1 cannot vanish identically, since it satisfies non-homogeneous Neumann boundary conditions on $\partial\Omega_j$, $j = 1, \ldots, N$, and therefore $u_1 > 0$. Suppose now that there exists $m < N$ such that $u_1 > 0, \ldots, u_{m-1} > 0$. Set

$$F_m(x, t, y) := -y \sum_{j=1}^{N} a_{m,j} u_j(x, t) + \frac{1}{2} \sum_{j=1}^{m-1} a_{j,m-j} u_j(x, t) u_{m-j}(x, t).$$

By the induction hypothesis, $F_m(x, t, 0) \geq 0$. Again, we can apply the comparison theorem to conclude that $u_m \geq 0$, and that either u_m vanishes identically, or $u_m > 0$. Suppose now by contradiction $u_m \equiv 0$. Replacing in (2), we obtain that $u_j u_{m-j} \equiv 0$ for $j = 1, \ldots, m$, contradicting the induction hypothesis.

The same argument applies for $m = N$. This achieves the proof. □

Remark 3.3 The existence of a positive solution, which could sound quite obvious from a biomedical point of view, is the fundamental mathematical requirement to be satisfied for our model to be considered sustainable.

Proposition 3.4 *We have $\tau_{\max} = +\infty$.*

Proof Suppose by contradiction $\tau_{\max} < +\infty$. Then, by Theorem 1 of Rothe (1984) (see also Theorem 7.1 in the Appendix)

$$\lim_{t \to \tau_{\max}} \|u(\cdot, t)\|_{(L^\infty(\Omega))^N} = +\infty.$$

Thus, we have to show that there exists $C > 0$ such that

$$\|u(\cdot, t)\|_{(L^\infty(\Omega))^N} \leq C \quad \text{for } t \in (0, \tau_{\max}).$$

We argue by induction on the components of u. Let $g \in \mathbf{C}^2(\bar{\Omega})$ be such that

$$\frac{\partial g}{\partial \nu} = 1 \quad \text{on } \partial\Omega_0$$

and

$$\frac{\partial g}{\partial \nu} = 1 \quad \text{on } \partial\Omega_j, \ j = 1, \ldots, M.$$

Without loss of generality, we may assume $g \geq 0$. We set $C := \max_{\bar{\Omega}} d_1 |\Delta_x g|$, $u_0 := g + Ct$ and $v_1 := u_1 - u_0$. We have

$$\begin{cases} \frac{\partial}{\partial t} v_1 = d_1 \Delta_x v_1 - v_1 \big(\sum_{j=2}^N a_{1,j} u_j + 2 a_{1,1} u_0 \big) \\ -a_{1,1} v_1^2 + d_1 \Delta_x u_0 - \frac{\partial u_0}{\partial t} - a_{1,1} u_0^2 - u_0 \sum_{j=2}^N a_{1,j} u_j \\ \frac{\partial v_1}{\partial \nu} = -1 \quad \text{on } \partial\Omega_0 \\ \frac{\partial v_1}{\partial \nu} = \psi_j - 1 \leq 0 \quad \text{on } \partial\Omega_j,\ j = 1, \ldots, M \\ v_1(x, 0) = U_1(x) - g(x), \quad x \in \Omega. \end{cases} \tag{11}$$

Set $h := -\big(\sum_{j=2}^N a_{1,j} u_j + 2 a_{1,1} u_0 \big) \leq 0$. Then

$$\begin{aligned} & d_1 \Delta_x v_1 - \frac{\partial}{\partial t} v_1 + h v_1 \\ & \quad = a_{1,1} v_1^2 - d_1 \Delta_x u_0 + C + a_{1,1} u_0^2 + u_0 \sum_{j=2}^N a_{1,j} u_j \\ & \quad \geq -d_1 \Delta_x u_0 + C \geq 0. \end{aligned}$$

By the parabolic maximum principle (Protter and Weinberger 1984, Theorem 7, p. 174), either $v_1 \leq 0$ in $[0, \tau]$ with $\tau < \tau_{\max}$, or its maximum on $[0, \tau]$ is attained on the parabolic boundary of $[0, \tau] \times \bar{\Omega}$. But the maximum cannot be attained on $(0, \tau] \times \partial\Omega$ by the parabolic boundary point lemma (Hopf's principle: see again Protter and Weinberger (1984), Theorems 6 and 7 p. 174), since $\frac{\partial v_1}{\partial \nu} \leq 0$ on $(0, \tau] \times \partial\Omega$. Thus

$$v_1 \leq \max\{0, U_1 - g\} \leq U_1,$$

and

$$0 \leq u_1 \leq U_1 + u_0 \leq \max_{\bar{\Omega}} (U_1 + g + C\tau_{\max}).$$

This proves that u_1 is bounded in $[0, \tau_{\max})$.

Suppose now

$$\|u_j(\cdot, t)\|_{(L^\infty(\Omega))^N} \leq C_j \quad \text{for } t \in (0, \tau_{\max})$$

$j = 1, \ldots, m-1$. If we choose $C \geq d_1 \max_{\bar{\Omega}} |\Delta_x u_0| + \frac{1}{2} \sum_{j=1}^{m-1} a_{j,m-j} C_j C_{m-j}$, $u_0 := g + Ct$ (where g is as above) and $v_m := u_m - u_0$,we have

$$\begin{cases} \frac{\partial}{\partial t} v_m = d_m \Delta_x v_m - v_m \sum_{j=1}^{N} a_{m,j} u_j \\ +d_m \Delta_x u_0 - \dfrac{\partial u_0}{\partial t} - u_0 \sum_{j=1}^{N} a_{m,j} u_j \\ +\frac{1}{2} \sum_{j=1}^{m-1} a_{j,m-j} u_j(x,t) u_{m-j}(x,t), \\ \frac{\partial v_m}{\partial \nu} = -1 \quad \text{on } \partial\Omega_0 \\ \frac{\partial v_m}{\partial \nu} = -1 \quad \text{on } \partial\Omega_j,\ j = 1, \dots, M \\ v_m(x,0) = -g(x), \quad x \in \Omega. \end{cases} \tag{12}$$

Set $h := -\sum_{j=1}^{N} a_{m,j} u_j \le 0$. Then

$$\begin{aligned} & d_m \Delta_x v_m - \frac{\partial}{\partial t} v_m + h v_m \\ & = -d_m \Delta_x u_0 + \frac{\partial u_0}{\partial t} + u_0 \sum_{j=1}^{N} a_{m,j} u_j \\ & \quad -\frac{1}{2} \sum_{j=1}^{m-1} a_{j,m-j} u_j(x,t) u_{m-j}(x,t) \\ & \ge C - d_m \Delta_x u_0 - \frac{1}{2} \sum_{j=1}^{m-1} a_{j,m-j} u_j(x,t) u_{m-j}(x,t) \\ & \ge C - d_m |\Delta_x u_0| - \frac{1}{2} \sum_{j=1}^{m-1} a_{j,m-j} C_j\, C_{m-j} \\ & \ge 0, \end{aligned}$$

and we can conclude as above.

Finally, the case $m = N$ can be treated in an almost analogous way (here $h \equiv 0$). □

We prove now a few asymptotic estimates. Their purpose is not inconsistent with the choice of modeling the early stage of the disease, but is due to different choices of the time scale. Roughly speaking, following Meyer-Luehmann et al. (2008), we can think of an observation interval *in vivo* of few weeks (the early stage of the disease), whereas the crucial interval from the onset of the disease up to the formation of senile plaques can be of the order of hours. Since we want to describe in full detail the very early stage of the disease, in the mathematical model we have to represent the period of few hours by an interval of unitary (say) length. Thus, the observation interval of weeks turns out to be a very long interval in the "mathematical time". Since we see, from the numerical simulation, that the biological parameters we are tracing (for instance the concentrations of different polymers) tend asymptotically to stabilize, from the modeling point of view such a long interval can be identified, for sake of simplicity, with an infinite interval.

Proposition 3.5 *For any $T > 0$ we have*

$$\lambda_T := \inf_{(T,\infty)\times\Omega} u_N > 0. \tag{13}$$

Moreover

$$\phi_N(t) := \fint_\Omega u_N(t,x)\,dx \to \ell \in (0,\infty] \quad \text{as } t \to \infty. \tag{14}$$

Proof First of all, we notice that

$$d_N \Delta u_N - \frac{\partial u_N}{\partial t} \le 0,$$

so that the maximum principle applies to $-u_N$ (Protter and Weinberger (1984), Chapter 3, Theorems 5 and 6). On the other hand, by Lemma 3.2, $\min_{\bar\Omega} u_N(T,\cdot) > 0$. Take now $t > T$ arbitrary. Again, the parabolic maximum principle yields that the minimum of u_N on $[T,t]\times\bar\Omega$ is attained at the time T. Indeed, it cannot be attained at point of $\partial\Omega$, by Protter and Weinberger (1984), Chapter 3, Theorem 6, since the normal derivative of u_N vanishes on the boundary of Ω. Then, by Protter and Weinberger (1984), Chapter 3, Theorem 5, it must coincide with the minimum at $t = T$, so that $\min_{[T,t]\times\bar\Omega} u_N = \min_{\bar\Omega} u_N(T,\cdot) > 0$ and (13) follows.

As for (14), it is easy to see that ϕ_N is a continuously differentiable function If $t > 1$, integrating (3) on Ω, and using the divergence theorem we get

$$\begin{aligned}\phi_N'(t) &= d_N \fint_\Omega \Delta u_N\,dx + \frac{1}{2}\sum_{j+k\ge N, j<N, k<N} a_{j,k} \fint_\Omega u_j u_k\,dx \\ &= \frac{1}{2}\sum_{j+k\ge N, j<N, k<N} a_{j,k} \fint_\Omega u_j u_k\,dx > 0.\end{aligned} \tag{15}$$

Then the assertion follows. □

Remark 3.6 Since, in our model, $u_N(t,\cdot)$ describes the plaques, then (13) states basically that plaques form extraordinarily quickly. This corresponds to the experimental evidences presented in Meyer-Luehmann et al. (2008).

Proposition 3.7 *If we set*

$$\Phi(t) := \sum_{m=1}^{N-1} \fint_\Omega m u_m(t,x)\,dx$$

(in other words, Φ is the total mass of soluble oligomers), then there exists $a > 0$ such that for $t > 1$we have

$$\Phi(t) \le e^{-a\lambda_1(t-1)}\Phi(1) + \frac{d_1 \sum_{j=1}^{M} \int_{\partial\Omega_j} \psi_j \, d\mathcal{H}^{n-1}}{a\lambda_1 |\Omega|}(1 - e^{-a\lambda_1(t-1)}). \tag{16}$$

Remark 3.8 Here $\mathcal{H}^{n-1}$ is the $(n-1)$-dimensional Hausdorff measure concentrated on $\partial\Omega_j$ for $j = 1, \dots, M$. In other words, if $n = 2$, then $\mathcal{H}^1$ is the length measure on the boundaries of the sets Ω_j, and, if $n = 3$, then $\mathcal{H}^2$ is the surface measure on the boundaries of the sets Ω_j.

Proof If $m = 1, \dots, N-1$, we multiply by m the equation for u_m in (1) and (2) and we sum up for $m = 1, \dots, N-1$. We obtain

$$\begin{aligned}\frac{\partial}{\partial t}\sum_{m=1}^{N-1} m u_m &= \Delta_x \sum_{m=1}^{N-1} d_m m u_m \\ &\quad - \sum_{m=1}^{N-1}\sum_{j=1}^{N} m a_{m,j} u_m u_j + \frac{1}{2}\sum_{m=2}^{N-1}\sum_{j=1}^{m-1} m a_{j,m-j} u_j u_{m-j} \\ &\le \Delta_x \sum_{m=1}^{N-1} d_m m u_m - \sum_{m=1}^{N-1} m a_{m,N} u_m u_N. \end{aligned} \tag{17}$$

Now, integrating (17) for $x \in \Omega$, keeping in mind the boundary conditions on $\partial\Omega$, we get, by the divergence theorem,

$$\begin{aligned}\frac{\partial}{\partial t}\int_\Omega \sum_{m=1}^{N-1} m u_m \, dx &\le d_1 \sum_{j=1}^{M} \int_{\partial\Omega_j} \psi_j \, d\mathcal{H}^{n-1} \\ &\quad - \sum_{m=1}^{N-1} \int_\Omega m a_{m,N} u_m u_N \, dx. \end{aligned} \tag{18}$$

Set now $a := \min\{a_{m,N}, m = 1, \dots, N-1\} > 0$. By (13), if $t > 1$, from (18) we have

$$\frac{\partial}{\partial t}\int_\Omega \sum_{m=1}^{N-1} m u_m \, dx \le d_1 \sum_{j=1}^{M} \int_{\partial\Omega_j} \psi_j \, d\mathcal{H}^{n-1} - a\lambda_1 \int_\Omega \sum_{m=1}^{N-1} m u_m \, dx, \tag{19}$$

and then (16) follows. □

Remark 3.9 The numerical simulations presented below suggest that the estimate (16) can be considered asymptotically optimal, in the sense that the numerical experiments show that there exist positive constants $\ell_1, \dots, \ell_{N-1}$ such that

$$\fint_\Omega m u_m(t, x) \, dx \to \ell_m \quad \text{as } t \to \infty,$$

for $m = 1, \dots, N-1$.

Alternatively, the following estimate for the total mass of the monomers can be proved.

Proposition 3.10 *If we set*

$$\phi_1(t) := \fint_\Omega u_1(t,x)\,dx,$$

then, for large t,

$$0 < \phi_1^2(t) < \frac{d_1}{a_{1,1}|\Omega|} S,$$

where

$$S := \sum_{j=1}^{M} S_j \quad \text{and} \quad S_j := \int_{\partial\Omega_j} \psi_j \, d\mathcal{H}^{n-1}.$$

Proof It is easy to see that ϕ_1 is a continuously differentiable function and that, by the divergence theorem,

$$\begin{aligned}
\phi_1'(t) &= d_1 \fint_\Omega \Delta u_1 \, dx - a_{1,1} \fint_\Omega u_1^2 \, dx - \sum_{j=2}^{N} a_{1,j} \fint_\Omega u_1 u_j \, dx \\
&= \frac{d_1}{|\Omega|} \sum_{j=1}^{M} S_j - a_{1,1} \fint_\Omega u_1^2 \, dx - \sum_{j=2}^{N} a_{1,j} \fint_\Omega u_1 u_j \, dx \\
&= a_{1,1}\Big(S - \fint_\Omega u_1^2 \, dx\Big) - \sum_{j=2}^{N} a_{1,j} \fint_\Omega u_1 u_j \, dx. \qquad (20)
\end{aligned}$$

In particular, by Cauchy–Schwarz inequality,

$$\phi_1'(t) \le a_{1,1}\Big(S - \phi_1^2(t)\Big) - \sum_{j=2}^{N} a_{1,j} \fint_\Omega u_1 u_j \, dx. \qquad (21)$$

Suppose first $\phi_1(0) > \sqrt{S}$. Then $\phi_1'(t) < 0$ as long as $\phi_1(t) > \sqrt{S}$. Set $T := \sup\{t > 0;\, \phi_1(s) > \sqrt{S},\, s \in [0,t)\}$. We want to show that $T < \infty$ and that $\phi_1(t) < \sqrt{S}$ in a right neigborhood of T. Suppose by contradiction $T = \infty$. By Proposition 3.5, for $t > 1$,

$$\fint_\Omega u_1 u_N \, dx \ge \lambda_1 \phi_1(t) \ge \lambda_1 \sqrt{S} > 0.$$

Therefore $\phi_1'(t) \leq -a_{1,N}\lambda_1\sqrt{S}$ and therefore $\lim_{t\to\infty}\phi_1(t) = -\infty$, yielding a contradiction.

Clearly $\phi_1(T) = \sqrt{S}$, so that $\phi_1'(T) \leq -\sum_{j=2}^{N} a_{1,j} \fint_\Omega u_1 u_j\, dx < 0$, by Lemma 3.2, so that $\phi_1(t) < \sqrt{S}$ in a right neighborhood of T. The same argument yields that $\phi_1(t) < \sqrt{S}$ when $t > T$. Indeed, if $T_1 := \sup\{t > T;\, \phi_1(s) < \sqrt{S}, s \in [T, t)\} < \infty$, we have $\phi_1(T_1) = \sqrt{S}$, $\phi_1'(T_1) < 0$, a contradiction.

If $\phi_1(0) < \sqrt{S}$, it is enough to repeat the last part of the argument.

Finally, if $\phi_1(0) = \sqrt{S}$ and $\phi_1'(0) \neq 0$, we fall again in one of the previous cases. Thus, we are left with the case $\phi_1(0) = \sqrt{S}$ and $\phi_1'(0) = 0$. Replacing $\phi_1'(0) = 0$ in (20) and taking into account that $u_m(0, \cdot) = 0$ when $m > 1$, we obtain that

$$\fint_\Omega u_1(0, x)^2\, dx = S = \left(\fint_\Omega u_1(0, x)\, dx\right)^2.$$

But this is possible only if $u_1(0, x) \equiv$ const., that contradicts the Neumann condition on $\partial\Omega_j$, $j = 1, \ldots, M$. □

4 Numerical scheme

The most important simplification made in the numerical simulations below is to consider bidimensional problems ($n = 2$). This is certainly not realistic, but it is enough to obtain qualitative information on the distribution of Aβ.

The model proposed in Sect. 2 takes into account M neurons, so the domain Ω had M holes. In order to make the numerical simulations and in particular the description of the geometry easier, we assume that the neurons are periodically distributed, so the boundary value problem becomes periodic, and it is enough to focus on a box around a single neuron.

Therefore, we look for periodic solutions $u_m(t, \cdot)$ in the plane, and the physical domain Ω is a period perforated by a single disk Ω_1, standing for the neuron. A more precise description of the geometry of the neuron could be achieved with the method described below, but it did not seem necessary at this exploratory stage. The production of the monomers in a small portion of the neuronal membrane is modeled by a non homogeneous and constant Neumann condition $\psi \geq 0$ supported in a small region of $\partial\Omega_1$. Periodicity boundary conditions are imposed on the lateral parts of $\partial\Omega$.

We have chosen to partition the domain Ω into periodic unstructured meshes made of triangles. This makes it possible to complexify the geometry if needed. In particular, with triangular meshes, one could as well simulate the model described in Sect. 2. Yet, more complex geometries with several neurons would require finer meshes and an increased computational cost.

Our strategy is to use piecewise linear finite elements to discretize the spatial variations of the concentrations, and standard semi-implicit Euler finite difference schemes for the variations w.r.t. time.

Consider an increasing sequence $(t_n)_{n=0,\ldots N_T}$, such that $0 = t_0 < t_1 < \cdots < t_{N_T} = T$. Call $\Delta t_n = t_{n+1} - t_n$. Let $\mathcal{T}_h$ be a family of periodic triangular meshes of the

domain Ω. The number h stands for the maximal diameter of the triangles in $\mathcal{T}_h$. We make a regularity assumption, i.e. that the angles of the triangles are bounded from below by a fixed constant.

The functions $x \to u_m(x, t_i), 0 \leq i \leq N_T, 1 \leq m \leq N$, will be approximated by continuous, periodic functions, affine on the triangles of $\mathcal{T}_h$. We call V_h the space

$$V_h = \{v \in \mathcal{C}^0_{\text{per}}(\Omega);\, v|_\tau \in \mathcal{P}_1, \quad \forall \tau \in \mathcal{T}_h\}.$$

Let $(\xi_i)_{1\leq i\leq N_h}$ be the vertices of the triangles of $\mathcal{T}_h$. The nodal basis $(\phi_i)_{1\leq i\leq N_h}$ is defined by $\phi_i(\xi_j) = \delta_{i,j}, \forall j, 1 \leq j \leq N_h$. Let $u^n_m \in V_h$ be the discrete versions of $x \to u_m(x, t_n)$ for $m = 1, \ldots, N$. We expand these functions on the nodal basis of V_h as follows:

$$u^n_m = \sum_{i=1}^{N_h} u^n_{m,i}\phi_i.$$

We use a first order semi-implicit time scheme: the diffusion is treated implicitly whereas the aggregation is treated explicitly. Therefore, at each time step, we need to solve a system of linear of the form:

$$\begin{aligned}
(M + \Delta t_n A_1)U^{n+1}_1 &= M(U^n_1 + \Delta t_n F^n_1) + \Delta t L^{n+1}_1,\\
(M + \Delta t_n A_m)U^{n+1}_m &= M(U^n_m + \Delta t_n F^n_m), \quad 2 \leq m \leq N-1,\\
(M + \Delta t_n A_N)U^{n+1}_N &= M(U^n_N + \Delta t_n W^n),
\end{aligned}$$

where $U^n_m = (u^n_{m,1}, \ldots, u^n_{m,N_h})^T \in \mathbb{R}^{N_h}$, M is the mass matrix : $M_{i,j} = \int_\Omega \phi_i\phi_j$, A_m is the stiffness matrix associated with the aggregates of size m : $A_{m,i,j} = d_m \int_\Omega \nabla\phi_i \cdot \nabla\phi_j$, and $F^n_m \in \mathbb{R}^{N_h}$, $W^n \in \mathbb{R}^{N_h}$ are the vectors whose coordinates are

$$F^n_{m,i} = -u^n_{m,i}\left(\sum_{\ell=1}^{N-1} a_{m,\ell}u^n_{\ell,i} + a_{m,N}u^n_{N,i}\right) + \frac{1}{2}\sum_{\ell=1}^{m-1} a_{\ell,m-\ell}u^n_{\ell,i}u^n_{m-\ell,i},$$

and

$$W^n_i = \frac{1}{2}\sum_{j+\ell\geq N, 1\leq j,\ell<N} a_{j,\ell}u^n_{j,i}u^n_{\ell,i},$$

and L^{n+1}_1 is the vector containing the Neumann data, which we do not write explicitly here. Standard arguments show that this discretization is second order with respect to the spatial variable x and first order with respect to time. Of course, higher order semi-implicit time schemes are possible.

Remark 4.1 Note that the explicit scheme taking account the aggregation has a conservative form: indeed, introducing $g^n_{m,i} = m u^n_{m,i}$ and $\tilde{F}^n_{m,i} = m F^n_{m,i}$, we can easily check that

$$\begin{aligned}\tilde{F}^n_{m,i} &= -a_{m,N} u^n_{N,i} g^n_{m,i} - g^n_{m,i} \sum_{\ell=1}^{N-1} a_{m,\ell} u^n_{\ell,i} + \frac{m}{2} \sum_{\ell=1}^{m-1} a_{\ell,m-\ell} u^n_{\ell,i} u^n_{m-\ell,i} \\ &= -a_{m,N} u^n_{N,i} g^n_{m,i} - J^n_{m+1/2,i} + J^n_{m-1/2,i}\end{aligned}$$

where

$$J^n_{m+1/2,i} = \sum_{j=1}^{m} \sum_{m-j+1}^{N-1} j a_{j,k} u^n_{j,i} u^n_{k,i} = \sum_{j=1}^{m} \sum_{m-j+1}^{N-1} \frac{a_{j,k}}{k} g^n_{j,i} g^n_{k,i}.$$

Thus the scheme reads

$$\begin{aligned}(M + \Delta t_n A_1) G^{n+1}_1 &= M(G^n_1 - \Delta t_n (J^n_{3/2} + K^n_1)) + L^n_1, \\ (M + \Delta t_n A_m) G^{n+1}_m &= M(G^n_m - \Delta t_n (J^n_{m+1/2} - J^n_{m-1/2} + K^n_m)), \quad 2 \le m \le N-1, \\ (M + \Delta t_n A_N) U^{n+1}_N &= M(U^n_N + \Delta t_n W^n),\end{aligned}$$

where

$$K^n_{m,i} = a_{m,N} u^n_{N,i} g^n_{m,i}.$$

Remark 4.2 Proceeding as in Filbet and Laurençot (2004a), it is possible to prove a stability condition for Δt_n involving $(U^n_m)_{m=1,\dots,N}$ such that the vectors $(U^{n+1}_m)_{m=1,\dots,N}$ have nonnegative entries. For keeping the paper short, we do not discuss this here. Under this condition, it is also possible to prove that the mass $\sum_{m=1}^{N-1} m(MU^n_m, 1)_2$ remains smaller than the quantity of monomer injected at the Neumann boundary between $t = 0$ and $t = t_n$.

5 Numerical simulation

Our model does not attempt to describe cellular injuries and the subsequent dementia, the most observed clinical stage of the disease that extends over several years. Therefore, the model we present should be considered reliable only for short (biological) times. Indeed it is only meant to describe the early stage of the disease at the cell level, and, in particular, its onset, which can be extremely quick as pointed out experimentally in Meyer-Luehmann et al. (2008). On the other hand, as we stressed above before the asymptotic estimates of Sect. 3, from the modelling point of view, short "biological times" become large "mathematical times", i.e. the time is rescaled in order to emphasize the qualitative behavior of the solutions.

We stress again that the numerical simulations presented below do not aim at the quantitative recovery of clinical data (that is far from our current reach), but rather at producing qualitative outputs that may underline interesting features of the phenomena, in particular asymptotic behaviors, in the light of what discussed above.

In our numerical simulations, we have taken the same diffusion coefficient for the first N_1 polymers (i.e. $d_1 = d_2 = \cdots = d_{N_1} := 1$), and $d_m = 0$ for $m > N_1$. We have taken $a_{i,j} = \alpha \frac{1}{ij}$ for $i, j < N$

In addition, we have slightly modified the model to more closely fit some clinical evidences, as follows: we have assumed the existence of a threshold $\kappa > 0$ such that

- as long as the global amount of soluble amyloid remains below κ, the production of Aβ from the membrane is positive;
- when this amount exceeds κ, the neuron dies and consequently the production stops.

This can be modelled as follows: there exists $N_0 < N$ such that the oligomers of length $1 \leq m \leq N_0$ are soluble (and therefore highly toxic for neurons, as pointed out in Sect. 1: see for instance, Haass and Selkoe (2007) and Walsh and Selkoe (2007)). Then we replace the boundary conditions in (2) by

$$\frac{\partial u_1}{\partial \nu} = \psi_j \quad \text{on } \partial\Omega_j,\ j = 1, \ldots, M$$

as long as

$$\sum_{m=1}^{N_0} \fint_{\Omega} u_m(t, x)\, dx < \kappa,$$

whereas

$$\frac{\partial u_1}{\partial \nu} = 0 \quad \text{on } \partial\Omega_j,\ j = 1, \ldots, M \quad \text{for } t > t_\kappa$$

where t_κ is the first time such that

$$\sum_{m=1}^{N_0} \fint_{\Omega} u_m(t, x)\, dx \geq \kappa \quad \text{for} t = t_\kappa.$$

For sake of simplicity, assume $N_0 = N - 1$. Clearly, if

$$\Phi(t) := \sum_{m=1}^{N_0} \fint_{\Omega} u_m(t, x)\, dx$$

remains below the threshold κ, then nothing changes in our previous model: we expect that the concentration of soluble oligomers stabilizes, whereas the concentration of the

fibrillar form grows, and that we eventually obtain thick plaques. Equation (16) shows that we can expect this phenomenon if the functions ψ_j are "small". On the other hand, if $\Phi(t)$ reaches the critical value κ at the time t_κ (take, for instance, $t_\kappa = 1$, to use again (16) without cumbersome modifications), then $\Phi(t) \to 0$ exponentially as $t \to \infty$. Roughly speaking, we can then assume that the averages of $u_1(t, \cdot), \dots u_{N-1}(t, \cdot)$ vanish for large t, and therefore that the concentrations themselves vanish for large t. Then we go back to (15) and we obtain that the average of $u_N(t, \cdot)$ stabilizes for large t. In other words, the neuron dies, the production of Aβ stops, the concentration of soluble oligomers quickly vanishes, and the formation of plaques stabilizes.

Our simulations show that for fairly large times, the total amount of short assemblies (that we can identify with soluble oligomers) remains constant, see Fig. 2, whereas the amount of amyloid in fibril form blows up. However, we stress that when we consider u_N, i.e. the concentration of the amyloid in the fibrillar form, the qualitative graphs that we obtain must be interpreted.

In Fig. 1, we show a plaque grown near a neuron. It has been obtained by considering the higher level sets of $u_N(t, \cdot)$. We have chosen $N = 16$, $N_1 = 10$ in our simulations.

In Figs. 2 and 3 we show, respectively, the total mass of soluble oligomers of length 5 for low and high rate of production of Aβ-oligomers. In Fig. 2, the rate of production of Aβ in the monomeric form is low compared with the critical threshold κ. The production of the amyloid does not stop, but the total mass stabilizes around a positive value. On the contrary, in Fig. 3, due to the higher production of monomers, the neuron dies and the total mass of soluble oligomers vanishes quickly. This corresponds to the clinical experience of advanced AD. For instance, quoting from Ballard et al. (2011), "meta-analyses suggest that AD can be differentiated from other dementias by the detection of lower concentration of Aβ_{1-42} . . . ". Moreover, low concentration of Aβ_{42} in CSF (Celebral Splinal Fluid) is listed among diagnostic criteria and differential diagnosis of Alzheimer's disease from other dementias.

Our simulation thus show that if the concentration of soluble polymers attains the critical value, then the growth of the fibrils ceases quickly. On the other hand, when the critical threshold is not attained, the growth goes on for large times, but the rate remains very small, since only a very small production of monomers is compatible with the life of neurons. These results are in agreement with the arguments given above.

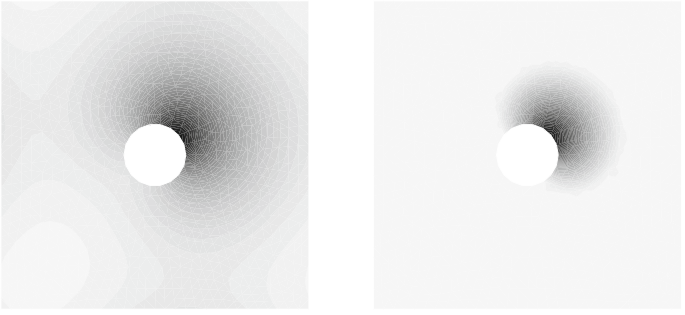

Fig. 1 Plaque generated with $N = 16$, $N_1 = 10$, $\alpha = 10$, $U_1 \equiv 0$, $\psi = 0.5$, $\kappa = 0.7$. Left: full plot. Right only the set $u > 0.3$ is presented, to show the shape of the senile plaque

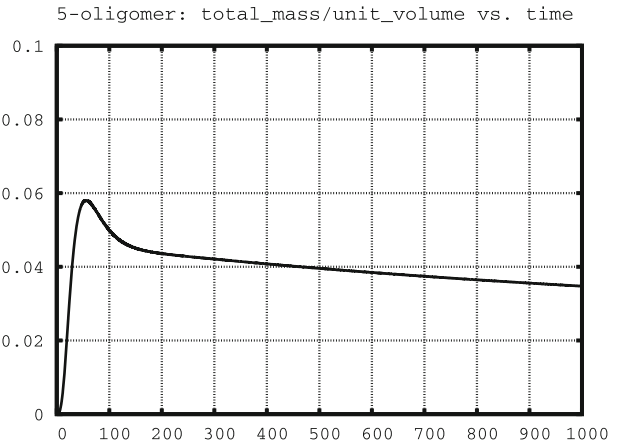

Fig. 2 Total mass of 5-oligomers with $N = 16$, $N_1 = 10$, $\alpha = 10$, $U_1 \equiv 0$, $\psi = 0.5$, $\kappa = 0.7$

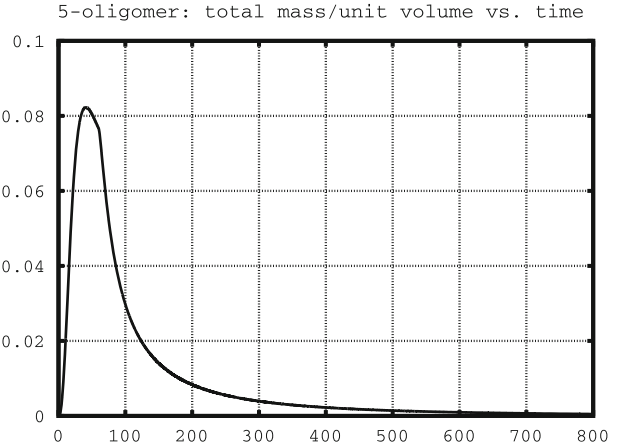

Fig. 3 Total mass of 5-oligomers with $N = 16$, $N_1 = 10$, $\alpha = 10$, $U_1 \equiv 0$, $\psi = 1$, $\kappa = 0.7$

To be more accurate from the mathematical point of view, one may think of replacing the average of $u_m(x, \cdot)$ on Ω by its average "near" the membrane $\partial\Omega$. However, we think that the implementation of this approach would be technically heavier and eventually would not yield a better model. This for several reasons, both mathematical and biological. First of all, our numerical simulation show that $u_m(x, \cdot)$ for small m is concentrated near $\partial\Omega$. Therefore, its average on a fixed neighborhood of $\partial\Omega$ is basically proportional (with an absolute proportionality constant) to the average on all Ω. In addition, the phenomenon leading ultimately to the neuronal apoptosis is not a simple contact effect, but involves a delicate sequence of actions "away from the membrane", like microglia activation and mobility, and subsequent action of the astroglia. Incidentally, we have stated that in this elementary model we deliberately ignore the effect of the glia.

It seems interesting to look at our results having in mind some comments in Haass and Selkoe (2007), p. 104. In a (very) rough way, we can summarize these comments as follows: modern Aβ enzyme-linked-immunosorbent assays (ELISAs) coupled with western blotting and mass spectrometry suggest that the plaque counting is a poor measure of the severity of the AD, and that levels of soluble Aβ, including soluble oligomers, correlate much better with the presence and degree of cognitive deficits than do simple plaque counts. Even more, "the idea that large aggregates of a disease causing protein can actually be inert or even protective to neurons has been supported by work on other protein folding disorders". These arguments seem to provide a possible interpretation of the case "below κ". Indeed, in this case, our model leads to the formation of senile plaques, but also to a low level of toxic soluble Aβ which is compatible with the absence of severe injury to neurons.

6 Comments

The aim of this note is not to improve or to simplify the results of Edelstein-Keshet and Spiross (2002) or of other contributions in biomathematics literature, but rather to raise the attention onto the important role of Smoluchowski equation in modelling the evolution of AD at the cell scale. In spite of the large literature concerning Smoluchowski equation in mathematics and physics, this equation does not seem to have been considered adequately in biomedical literature (with the exception of Murphy and Pallitto (2000)). It is also worth stressing that Smoluchowski equation is used in Murphy and Pallitto (2000) for modelling agglomeration *in vitro*. On the contrary, our model is meant to describe the evolution *in vivo*, and therefore we have to add the diffusion term, as well as the source term on the neuronal membrane. Since, in numerical simulation, the presence of the diffusion term makes computations much heavier, one could wonder whether we can drop this term. Mathematically, dropping the diffusion would mean, in our model, to take all the diffusion coefficients d_j, $j = 1, \ldots, N$, to be zero. But then Eq. (16) would yield an exponential decay of the total mass of the soluble oligomers, also in presence of the production of amyloid by sick but still alive neurons. In other words, the low level of amyloid in the CSF would be a general phenomenon, not related to the neuronal loss.

As explicitly stated in the title, we present here an"elementary" model, in the sense that we focus our attention on aggregation and diffusion of the β-amyloid, and deliberately ignore other biological phenomena, like the action of astrocytes and microglia on the diffusion (see again Meyer-Luehmann et al. (2008); Edelstein-Keshet and Spiross (2002); Quinlan and Straughan (2005)), as well as the interactions between different isoforms (Aβ_{40} and Aβ_{42}, see for instance Jan et al. (2008)).

Finally, it is worth stressing that the present model is closely related to the chosen scale, i.e. the scale of a single neuron. One could alternatively think of different scales and therefore of different models.

For instance, one could try to model the intra-membranous phenomena ultimately yielding the production of the toxic Aβ-amyloid. At such a scale, neither aggregation nor diffusion are relevant, and such an utterly different phenomenon should be described with totally different models. At the scale chosen in the present work, these

phenomena only appear through their final output, i.e. the production of the amyloid monomers that is modelled with a Neumann boundary condition.

Alternatively, one could describe a large portion of cerebral tissue during a longer time interval. Then other phenomena should be taken into account, like, for instance, the spreading of the malfunctioning of the Aβ production, the effect of the amyloid on healthy neurons, and eventually the neuronal death. Again, an utterly different phenomenon to be (if possible) described with other utterly different models.

Appendix

For the reader's convenience we collect some known results (see for instance Rothe (1984) Theorem 1 page 111 and Theorem 3 page 123), taylored according to our needs, used in the previous sections.

Let

$$F = F(t,u) : [0,\infty[\times\mathbb{R}^N \to \mathbb{R}^N$$

be such that:

- $F(\cdot,u)$ is measurable in $[0,\infty[$ for all $u \in \mathbb{R}^N$;
- F is locally bounded in $[0,\infty[\times\mathbb{R}^N$;
- F is locally lipschitz continuous in u uniformly in $t \in [0,T]$ for any $T > 0$.

Let $d_1 > 0, \ldots, d_N > 0$ denote the diffusion coefficients.

Let Ω be an open regular subset of $\mathbb{R}^n$. If $F = (F_1, \ldots, F_N)$ and $u = (u_1, \ldots, u_N) : \bar{\Omega} \to \mathbb{R}^N$, we consider the reaction-diffusion system

$$\frac{\partial u_j}{\partial t} = d_j \Delta u_j + F_j(t,u) \quad \text{for } t > 0 \text{ and } j = 1, \ldots, N \tag{22}$$

together with the boundary condition

$$\frac{\partial u_j}{\partial \nu} = 0 \quad \text{on } \partial\Omega, \tag{23}$$

and the initial condition

$$u(0,\cdot) = u_0. \tag{24}$$

Then the following theorems hold.

Theorem 7.1 *Let $u_0 \in \mathbf{C}^{2+\alpha}(\bar{\Omega})$ for some $\alpha \in (0,1)$ be such that*

$$\frac{\partial u_0}{\partial \nu} = 0 \quad \textit{on } \partial\Omega.$$

If for any (t,u) and (τ,v) in a bounded set $B \subset [0,\infty[\times\mathbb{R}^N$ we have

$$|F(t,u) - F(\tau,v)| \le C_B(|t-\tau|^{\alpha/2} + |u-v|),$$

then there exist $T_{\max} > 0$ *and* $u \in \mathbf{C}^{1+\alpha/2,2+\alpha}([0, T_{\max}) \times \bar{\Omega})$ *such that*

- *u satisfies* (22), (23), (24);
- $\lim_{t \to T_{\max}} \|u(t, \cdot)\|_{L^\infty(\Omega)} = \infty$.

Theorem 7.2 *If* $u, v \in \mathbf{C}^{1,2}([0, T] \times \bar{\Omega})$ *satisfy:*

- $u(0, \cdot) \leq v(0, \cdot)$;
- $\dfrac{\partial u}{\partial \nu} \leq \dfrac{\partial v}{\partial \nu}$ *in* $(0, T) \times \partial\Omega$;
- $\dfrac{\partial u_j}{\partial t} - d_j \Delta u_j - F_j(t, u) \leq \dfrac{\partial v_j}{\partial t} - d_j \Delta v_j - F_j(t, v)$ *in* Ω *for* $t \in (0, T)$ *and* $j = 1, \ldots, N$;

then either $u \equiv v$ *or* $u(t, \cdot) < v(t, \cdot)$ *in* $(0, T] \times \bar{\Omega}$.

References

Amann H (2000) Coagulation-fragmentation processes. Arch Ration Mech Anal 151(4):339–366

Amann H, Walker C (2005) Local and global strong solutions to continuous coagulation-fragmentation equations with diffusion. J Differ Equ 218(1):159–186

Amann H, Weber F (2001) On a quasilinear coagulation-fragmentation model with diffusion. Adv Math Sci Appl 11(1):227–263

Ballard C, Gauthier S, Corbett A, Brayne C, Aarsland D, Jones E (2011) Alzheimer's disease. Lancet 377:1019–1031

Bero AW, Yan P, Roh JH, Cirrito JR, Stewart FR, Raichle ME, Lee I-M, Holtzman DM (2011) Neuronal activity regulates the regional vulnerability to amyloid-β deposition. Nat Neurosci 14:750–756

Blennow K, de Leon MJ, Zetterberg H (2006) Alzheimer's disease. Lancet 368:387–403

Bourgade J-P, Filbet F (2008) Convergence of a finite volume scheme for coagulation-fragmentation equations. Math Comp 77(262):851–882

Chimon S, Shaibat MA, Jones CR, Calero DC, Aizezi B, Ishii Y (2007) Evidence of fibril-like [beta]-sheet structures in a neurotoxic amyloid intermediate of Alzheimer's [beta]-amyloid. Nat Struct Mol Biol 14(12):1157–1164

Cruz L, Urbanc B, Buldyrev SV, Christie R, Gmez-Isla T, Havlin S, McNamara M, Stanley HE, Hyman BT (1997) Aggregation and disaggregation of senile plaques in Alzheimer disease. Proc Natl Acad Sci USA 94(14):7612–7616

Drake RL (1972) A general mathematical survey of the coagulation equation. Topics in Current Aerosol Research (Part 2), International Reviews in Aerosol Physics and Chemistry. Pergamon Press, Oxford

Edelstein-Keshet L, Spiross A (2002) Exploring the formation of Alzheimer's disease senile plaques in silico. J Theor Biol 216(3):301–326

Filbet F, Laurençot P (2004) Mass-conserving solutions and non-conservative approximation to the Smoluchowski coagulation equation. Arch Math (Basel) 83(6):558–567

Filbet F, Laurençot P (2004) Numerical simulation of the Smoluchowski coagulation equation. SIAM J Sci Comput 25(6):2004–2028 (electronic)

Goodhill GJ (1997) Diffusion in axon guidance. Eur J Neurosci 9(7):1414–1421

Haass C, Selkoe DJ (2007) Soluble protein oligomers in neurodegeneration: lessons from the Alzheimer's amyloid beta-peptide. Nat Rev Mol Cell Biol 8(2):101–112

Hatzikirou H, Deutsch A, Schaller C, Simon M, Swanson K (2005) Mathematical modelling of glioblastoma tumour development: a review. Math Models Methods Appl Sci 15(11):1779–1794

Hill TL (1983) Length dependence of rate constants for end-to-end association and dissociation of equilibrium linear aggregates. Biophys J 44:285–288

Jan A, Gokce O, Luthi-Carter R, Lashuel HA (2008) The ratio of monomeric to aggregated forms of Aβ_{40} and Aβ_{42} Is an important determinant of amyloid-β aggregation, fibrillogenesis, and toxicity. J Biol Chem 283(42):28176–28189

Knowles TPJ, Waudby CA, Devlin GL, Cohen SIA, Aguzzi A, Vendruscolo M, Terentjev EM, Welland ME, Dobson CM (2009) An analytical solution to the kinetics of breakable filament assembly. Science 326(5959):1533–1537

Laurençot P, Mischler S (2002) Global existence for the discrete diffusive coagulation-fragmentation equations in L^1. Rev Mat Iberoam 18(3):731–745

Mattson MP (2004) Pathways towards and away from Alzheimer's disease. Nature 430:631–639

Meyer-Luehmann M, Spires-Jones TL, Prada C, Garcia-Alloza M, De Calignon A, Rozkalne A, Koenigsknecht-Talboo J, Holtzman DM, Bacskai BJ, Hyman BT (2008) Rapid appearance and local toxicity of amyloid-β plaques in a mouse model of Alzheimer's disease. Nature 451(7179):720–724

Meyer-Luhmann M (2004) Experimental approaches to study cerebral amyloidosis in a transgenic mouse model of Alzheimer's disease. PhD thesis, University of Basel, Faculty of Science, CH

Mischler S, Ricard MR (2003) Existence globale pour l'équation de Smoluchowski continue non homogène et comportement asymptotique des solutions. C R Math Acad Sci Paris 336(5):407–412

Murphy RM, Pallitto MM (2000) Probing the kinetics of [beta]-amyloid self-association. J Struct Biol 130(2–3):109–122

Nicholson C, Sykov E (1998) Extracellular space structure revealed by diffusion analysis. Trends Neurosci 21(5):207–215

Ono K, Condron MM, Teplow DB (2009) Structure-neurotoxicity relationships of amyloid beta-protein oligomers. Proc Natl Acad Sci 106(35):14745–14750

Protter MH, Weinberger HF. Maximum principles in differential equations. Springer-Verlag, New York, 1984 Corrected reprint of the 1967 original

Quinlan RA, Straughan B (2005) Decay bounds in a model for aggregation of microglia: application to Alzheimer's disease senile plaques. Proc R Soc Lond Ser A Math Phys Eng Sci 461(2061):2887–2897

Rothe F (1984) Global solutions of reaction-diffusion systems volume 1072 of Lecture Notes in Mathematics. Springer-Verlag, Berlin

Smoluchowski M (1917) Versuch einer mathematischen theorie der koagulationskinetik kolloider lsungen. IZ Phys Chem 92:129168

Tomsky SJ, Murphy RM (1992) Kinetics of aggregation of synthetic beta-amyloid peptide. Arch Biochem Biophys 294:630–638

Urbanc B, Cruz L, Buldyrev SV, Havlin S, Irizarry MC, Stanley HE, Hyman BT (1999) Dynamics of plaque formation in alzheimer's disease. Biophys J 76(3):1330–1334

Walsh DM, Selkoe DJ (2007) Aβ oligomers: a decade of discovery. J Neurochem 101(5):1172–1184

Wrzosek D (1997) Existence of solutions for the discrete coagulation-fragmentation model with diffusion. Topol Methods Nonlinear Anal 9(2):279–296

Xue W-F, Homans SW, Radford SE (2008) Systematic analysis of nucleation-dependent polymerization reveals new insights into the mechanism of amyloid self-assembly. PNAS 105:8926–8931